

ELECTRONIC SUPPLEMENTARY INFORMATION

**Development of New Lanthanide(III) Ion-Based Magnetic Affinity
Material for Phosphopeptide Enrichment**

Vahit Gök^a, Önder Topel^{a*}, Sevil Aksu^a

^a *Department of Chemistry, Faculty of Science, Akdeniz University, 07058, Antalya, Turkey*

* Corresponding author: ondertopel@akdeniz.edu.tr

1. Diethyl 4-bromopyridine 2,6-dicarboxylate synthesis (2)

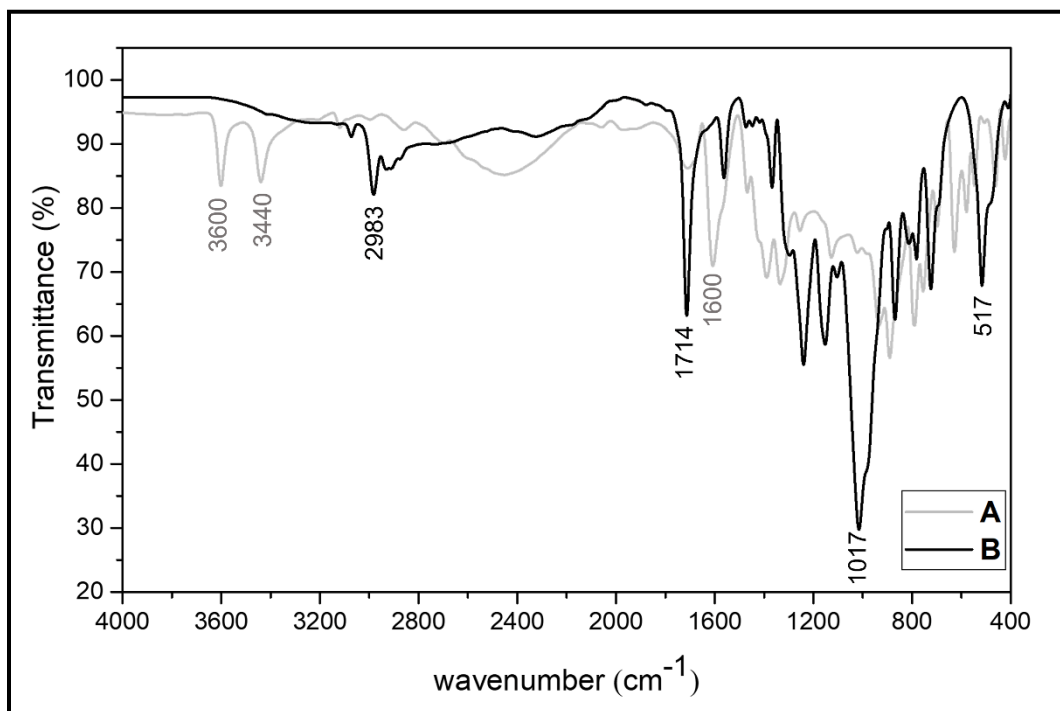


Fig. S1. FTIR spectrum of chelidamic acid (A) (1) and diethyl 4-bromopyridine 2,6-dicarboxylate (B)

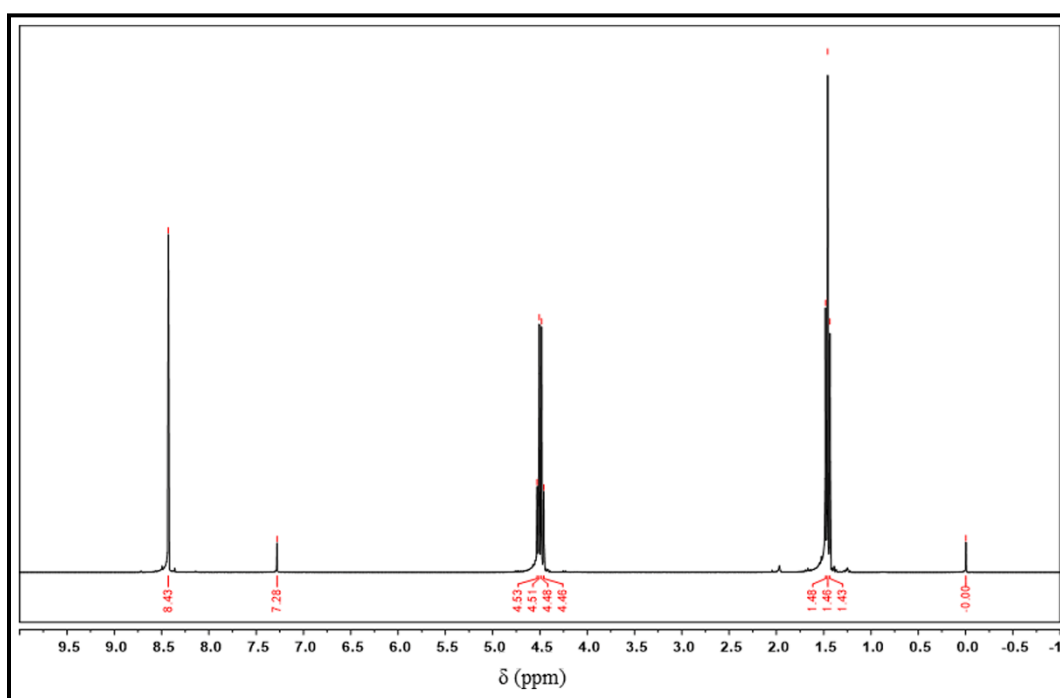


Fig. S2. ¹H-NMR spectrum of diethyl 4-bromopyridine 2,6-dicarboxylate (2)

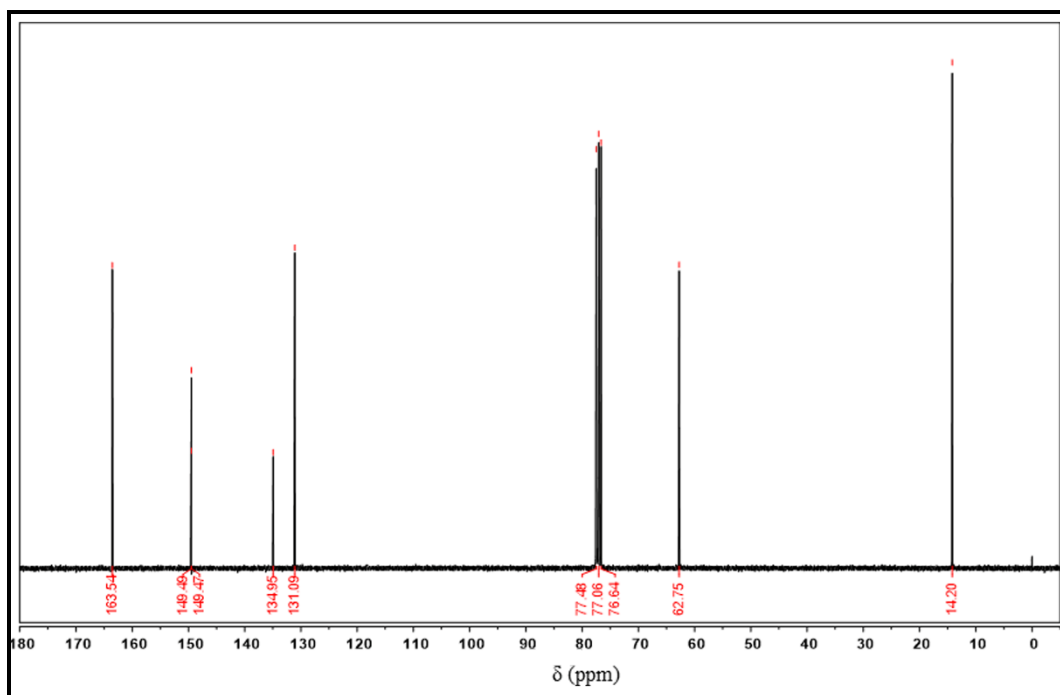


Fig. S3. ^{13}C -NMR spectrum of diethyl 4-bromopyridine 2,6-dicarboxylate (**2**)

The structure of the diethyl 4-bromopyridine 2,6-dicarboxylate ligand was characterized by ^1H and ^{13}C NMR measurements. The results are shown in Figs. S2 and S3, respectively. NMR results: ^1H -NMR (400 MHz, DMSO-d_6 , δ , mg.L^{-1}): 8.43 (s, ArCH); 4.50 (q, $J=9.5$ Hz, CH_2); 1.46 (t, $J=9.4$ Hz, CH_3). ^{13}C -NMR (100 MHz, DMSO-d_6 , δ , mg.L^{-1}): 163.54; 149.48 (q, $J=9.5$ Hz, ArCH_2), 135.131 (t, $J=9.5$ Hz, ArCH_3); 62.75; 14.2.

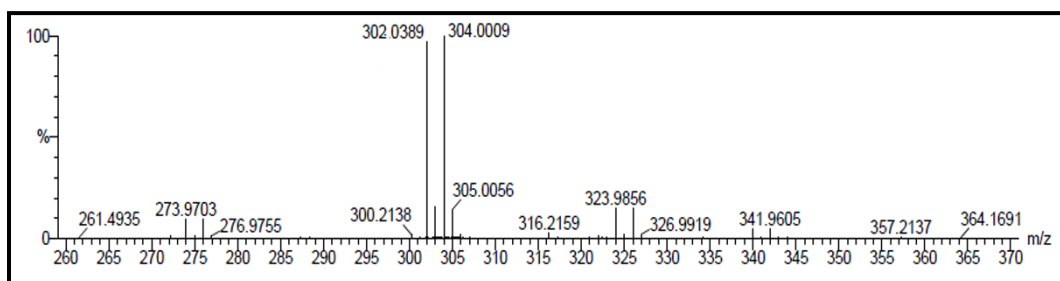


Fig. S4. MS spectrum of diethyl 4-bromopyridine 2,6-dicarboxylate (**2**)

2. Synthesis of the chelidamic acid-modified magnetic nanoparticles (6)

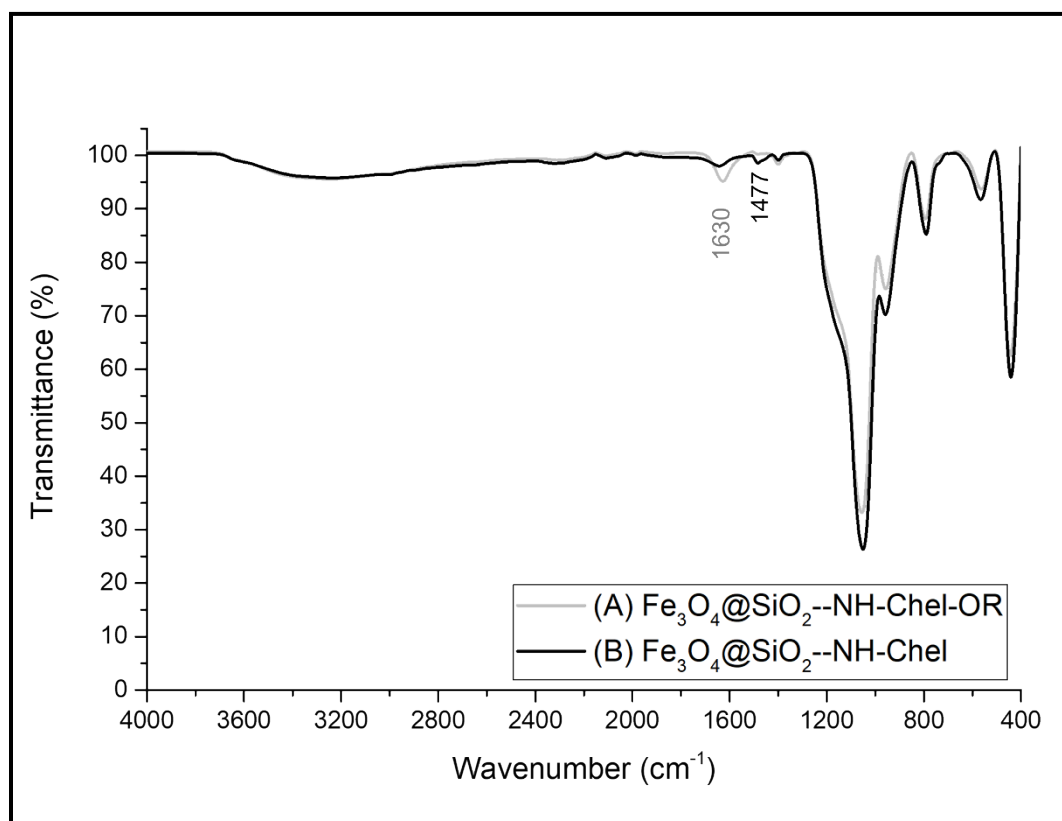


Fig. S5. FTIR spectra of diethyl 4-bromopyridine 2,6-dicarboxylate modified magnetic nanoparticles (A) and chelidamic acid modified magnetic nanoparticles (B) after hydrolysis

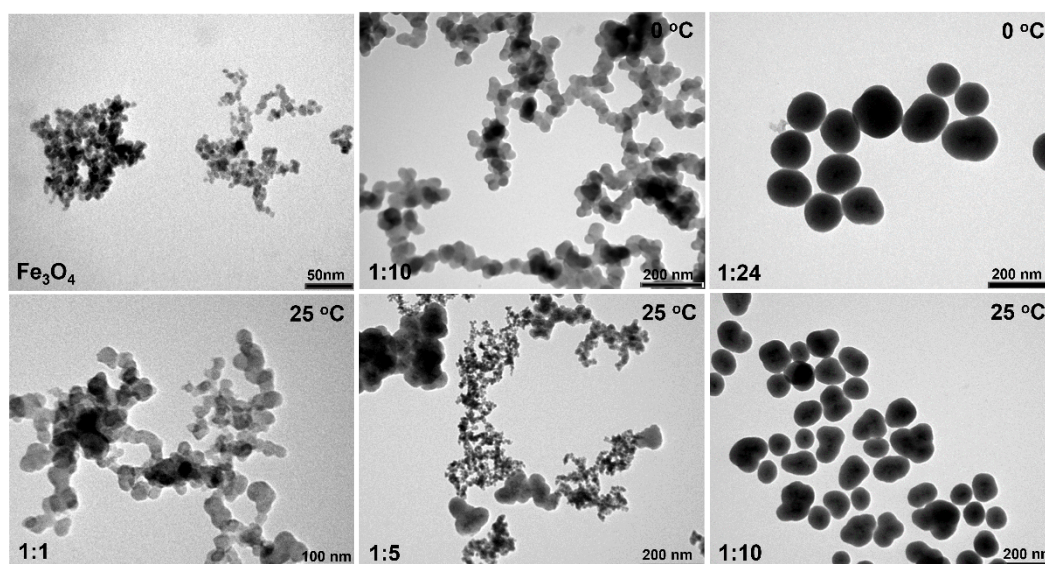


Fig. S6. Size and morphology change of silica-coated magnetic Fe_3O_4 nanoparticles based on the mole ratio of $(\text{FeO})_x:\text{SiO}_2$ and the reaction temperature

3. Phosphate adsorption studies of Ln³⁺-Mag-IMAC material

3.1. Spectroscopic determination of phosphate ion in aqueous solution

Phosphate ion adsorption studies were carried out in aqueous solution to model the suitability of the developed Ln³⁺-Mag-IMAC material for phosphopeptide enrichment processes. Spectrophotometric determination of phosphate ion concentration was performed according to standard Ammonium molybdate spectrometric method (ISO standard ISO6878:2004). In this method, the determination of phosphate ion concentration is based on the fact that orthophosphate ions form phosphomolibdate complex in acidic solution containing molybdate and antimony ions. A dense molybdenum blue is formed by reducing the resulting complex with ascorbic acid. The concentration of orthophosphate is determined by measuring the absorbance of the complex at 880 nm (ISO6878:2004 (E)). In the standard method, an acid reactive solution consisting 300 mL of 9 M H₂SO₄, 100 mL of 0.1 M ammonium heptamolybdate and 100 mL of 0.005 M antimony potassium tartrate is prepared which is stable up to 2 months in dark. Then, 100 mL of 0.5 M ascorbic acid solution was used as reducing agent which is stable for up to 2 weeks. When measuring phosphate concentration, 2 mL of the acid reactive solution and 1 mL of ascorbic acid were added to 1-10 mL of sample and diluted to 50 mL. The mixture was stirred for the fixed 10 min., then its absorbance was measured at 880 nm. This standard procedure was applied to all samples in the same way (ISO6878:2004 (E)).

At the beginning of the measurements, a calibration curve was created to determine the phosphate concentration. For this purpose, a series of standard phosphate solutions with concentrations of 10, 25, 75, 100, 150 and 200 mol.L⁻¹ were prepared. Then, their absorption spectra between 200-900 nm were measured according to the procedure described above with a Carry 100 UV/vis spectrophotometer. The spectra are given on the left in Fig. S6. The calibration curve (on the right side) was drawn using the corresponding absorbance values at 880 nm in the absorption spectra on the left in Fig. S6.

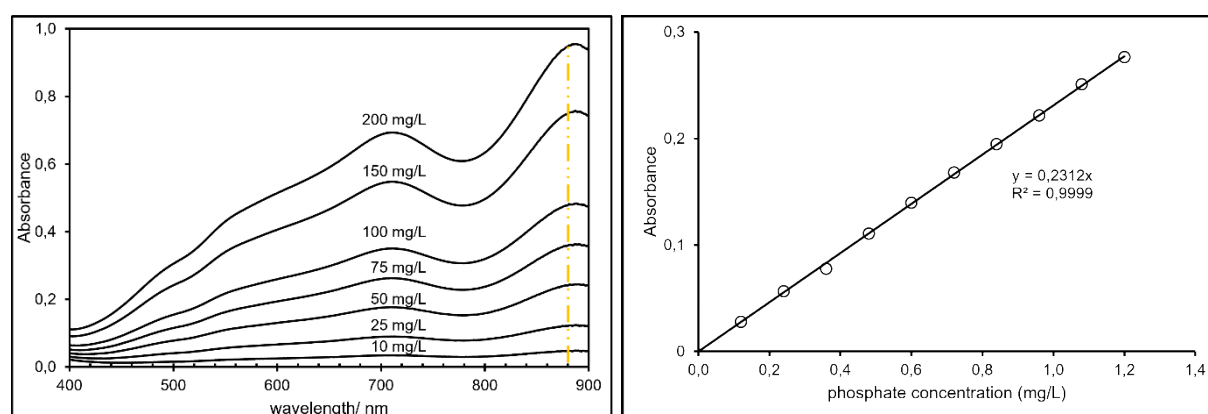


Fig. S7. Calibration curve (on the right) to determine phosphate concentration. The graph was drawn from the corresponding absorbance values to 880 nm in the concentration dependent UV/vis spectra (left)

3.2. Adsorption Studies

Batch adsorption experiments were performed to determine the phosphate adsorption performance of Ln³⁺-Mag-IMAC material at 25 °C. Centrifuge tubes including Ln³⁺-Mag-IMAC samples and phosphate solutions of 20 mL were shaken in Nüve ST 402 shaking water-bath at a constant shaking speed of 150 rpm . Adsorption isotherm experiments were conducted at pH 3 by mixing 5 mg of Ln³⁺-Mag-IMAC material with 20 mL phosphate solutions having different concentrations in the range of 5-100 mg.L⁻¹ for 48 h at 25°C. At the end of the time, the Ln³⁺-Mag-IMAC particles in the samples were centrifuged and the solution was filtered using a 0.20 µm membrane syringe filter to prepare it for phosphate analysis. The phosphate concentration in the samples was determined using the standard method at 880 nm by UV/vis spectrophotometer as described above. Then, the amount of adsorbed phosphate ion per gram of Ln³⁺-Mag-IMAC material at equilibrium time, *i.e.* the adsorption capacity at equilibrium, q_e (mol.g⁻¹), was calculated by Eq. (1):

$$q_e = \frac{(C_0 - C_e) \cdot V}{w} \quad (1)$$

where C_0 and C_e are the concentration of phosphate at initial time and equilibrium time, respectively (mol.L⁻¹), V is the volume of solution (L), w is the mass of Ln³⁺-Mag-IMAC (g). In this study, the adsorption data were the average of duplicate measurements and relative errors of the experimental data were less than 5%. Adsorption isotherms are given in Figs. S7 and S8 for Er³⁺-Mag-IMAC material and Dy³⁺-Mag-IMAC material, respectively.

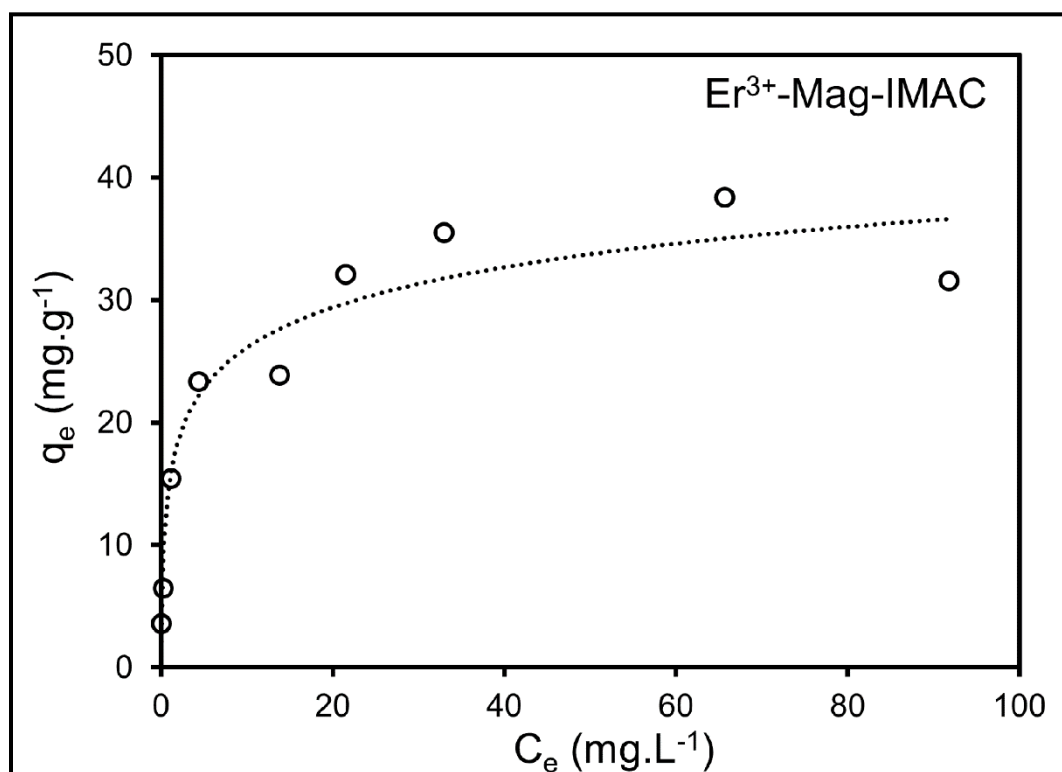


Fig. S8. Adsorption isotherms for the adsorption of phosphate ions onto Er³⁺-Mag-IMAC material at 25 °C (The dashed line shows Langmuir isotherm)

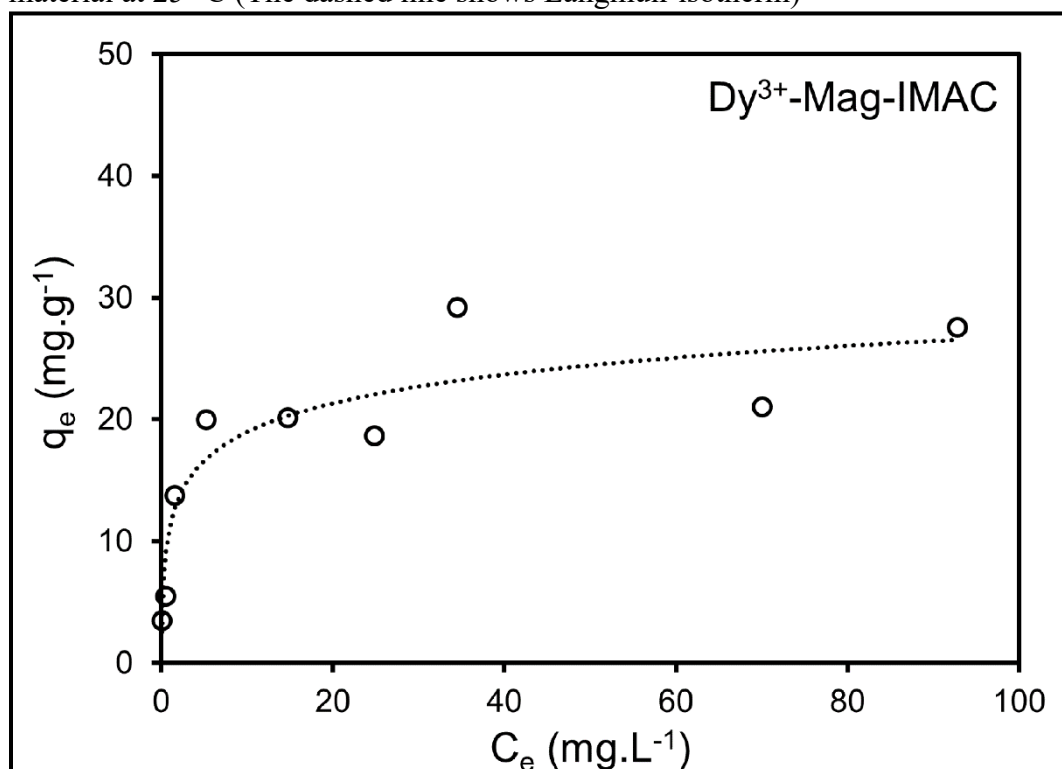


Fig. S9. Adsorption isotherms for the adsorption of phosphate ions onto Dy³⁺-Mag-IMAC material at 25 °C (The dashed line shows Langmuir isotherm)

To determine which isotherm best fits to the experimental data in Figs. S7 and S8, Langmuir, Freundlich and Temkin isotherm models in Table S1 were applied to the experimental data. From these models, the Langmuir model assumes that a monolayer adsorption takes place on a homogeneous adsorbent surface. According to the Freundlich model, a multilayer adsorption is carried out by a heterogeneous adsorbent surface. Adsorption isotherm parameters were calculated from C_e/q_e versus C_e plots for the Langmuir model, from $\ln q_e$ versus $\ln C_e$ plots for the Freundlich model and from q_e versus $\ln C_e$ plots for the Temkin model and are listed in Table S1. Determined isotherm parameters for each model applied were listed in Table S2. According to the r^2 values, the data for Ln³⁺-Mag-IMAC materials were best-fitted by the Langmuir isotherm model. This means that phosphate ion adsorption onto the developed Ln³⁺-Mag-IMAC materials is a monolayer adsorption process. The adsorption surface of developed Ln³⁺-Mag-IMAC materials is supposed to be homogeneous due to the affinity of lanthanide(III) ions on the surface of the developed Ln³⁺-Mag-IMAC materials to the phosphate ion. In addition, since lanthanide(III) ions on the surface present equivalent binding sites, adsorption energies should be equivalent to all adsorption sites. The K_L value expressed in the Langmuir isotherm model refers to the affinity between magnetic IMAC materials and phosphate. A higher K_L value indicates that higher adsorption occurs at lower phosphate concentrations.

Table S1. The most common used adsorption isotherms

Model	Equations	Definitions
Langmuir Isotherm ¹	$C_e/q_e = (C_e / q_{\max}) + 1 / K_L$	q_e is the amount of adsorbed dye by adsorbent at equilibrium ($\text{mol}\cdot\text{g}^{-1}$); C_e is the equilibrium concentration of adsorbate ($\text{mol}\cdot\text{L}^{-1}$); q_{\max} is the maximum adsorption capacity at monolayer coverage ($\text{mol}\cdot\text{g}^{-1}$); K_L is the adsorption equilibrium constant related to the energy of adsorption ($\text{L}\cdot\text{g}^{-1}$)
Freundlich Isotherm ²	$\ln q_e = \ln K_F + (1/n)\ln C_e$	K_F is a Freundlich constant representing the adsorption capacity ($(\text{mol}\cdot\text{g}^{-1})(\text{L}\cdot\text{mol}^{-1})^{1/n}$); n is a constant depicting the adsorption intensity
Temkin Isotherm ³	$q_e = K_1 \ln K_2 + K_1 \ln C_e$	K_1 is the Temkin isotherm energy constant ($\text{L}\cdot\text{mol}^{-1}$) and K_2 is the Temkin isotherm constant

¹ I. Langmuir, The constitution and fundamental properties of solid and liquids -Part I, Solids. Journal of the American Chemical Society, 40 (1918) 1361 -1403.

² H. Freundlich, Über die Adsorption in Lösungen. Zeitschrift für Physikalische Chemie, 57 (1906) 385 -471.

³M.I. Temkin, V. Pyzhev, Kinetics of ammonia synthesis on promoted iron catalyst. Acta Physico Chimica USSR, 12 (1940) 327 -356.

Table S2. Adsorption isotherm parameters of Langmuir, Freundlich and Temkin equations and correlation coefficients for the adsorption of phosphate ion onto Ln^{3+} -Mag-IMAC at 25°C.

Langmuir parameters			
Material	q_{\max} ($\text{mg}\cdot\text{g}^{-1}$)	K_L ($\text{L}\cdot\text{g}^{-1}$)	r^2
Er ³⁺ -Mag-IMAC	34.13	25.97	0.9838
Dy ³⁺ -Mag-IMAC	28.17	8.540	0.9814
Freundlich parameters			
Material	$K_F ((\text{mg}\cdot\text{g}^{-1})\cdot(\text{L}\cdot\text{mg}^{-1})^{1/n})$	$1/n$	r^2
Er ³⁺ -Mag-IMAC	9.80×10^{-4}	2.956	0.9299
Dy ³⁺ -Mag-IMAC	20.5×10^{-4}	3.017	0.8716
Temkin parameters			
Material	K_1 ($\text{L}\cdot\text{g}^{-1}$)	K_2	r^2
Er ³⁺ -Mag-IMAC	4.743	24.545	0.9319
Dy ³⁺ -Mag-IMAC	3.400	27.854	0.8458

3.3. pH Effect on adsorption of phosphate ions on Ln³⁺-Mag-IMAC material

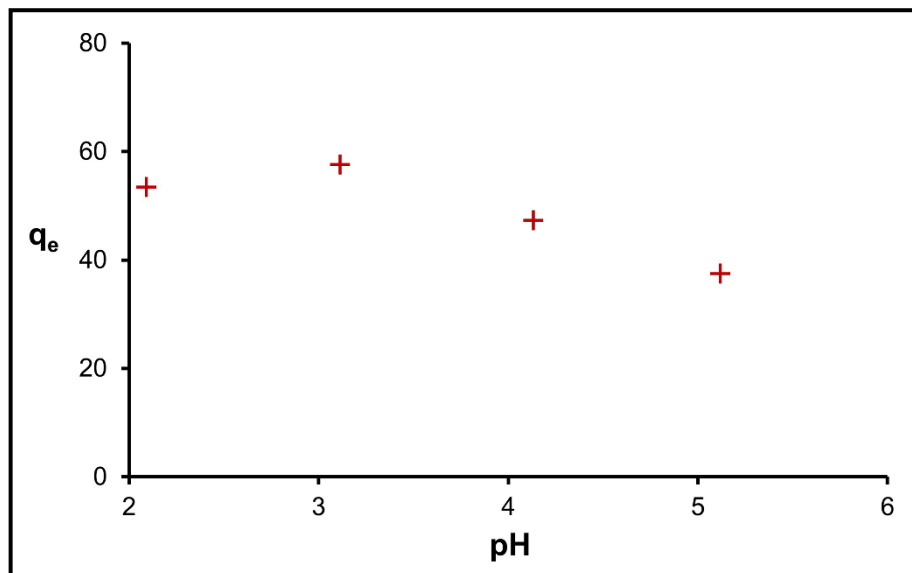


Fig. S10. Change of phosphate adsorption on developed Er³⁺-Mag-IMAC material depending on pH